Alternative Control Logic for Type-II Variable-Stiffness System

Junjiro Onoda* and Kenji Minesugi†
Institute of Space and Astronautical Science, Sagamihara, Kanagawa 229, Japan

Introduction

VIBRATION suppression of space structures is an important and difficult problem because in many cases their damping is expected to be low while the shape accuracy requirement is stringent. An attractive approach for the problem is the active vibration suppression. Numerous works have been published on the subject with various types of actuators. In most of these works, the control forces or moments are directly applied to the structures. But another approach, vibration suppression by stiffness control, has also been studied by several researchers.

To suppress the lateral vibration of tension-stabilized structures, Chen[1] proposed to control their tension. Because the lateral stiffness of the tension-stabilized structures is proportional to its tension, his work suggests that the vibration can be suppressed by varying the stiffness. Fanson et al.[2] showed that the two-degree-of-freedom vibration of a variable-stiffness system can also be suppressed by the stiffness control. Later, Onoda et al.[3] introduced another type of variable-stiffness system, which was referred to as type-II, whereas the known variable-stiffness system was called type-I in the paper. Unlike type-I, type-II variable-stiffness elements cannot supply the system any energy. Therefore, structures with them are always stable even if their stiffness are improperly controlled. Furthermore, they proposed several types of control logic to suppress the vibration of a multi-degree-of-freedom (MDOF) system by controlling the stiffness of multiple type-II variable-stiffness elements. The vibration suppression performance of a controlled type-II variable-stiffness system was demonstrated by both numerical simulations and an experiment. Recently, Minesugi[4] proposed another type of control logic based on the energy transfer between the modes due to the stiffness variation, although its application to the system with multiple variable-stiffness elements was still left as a future work.

In this Note, suggested from the linear quadratic (LQ) control, another new type of on-off control logic is proposed for the MDOF system with multiple type-II variable-stiffness truss members. The performance of the new approach is studied by applying it to a beam-like truss example, and it is compared with the approaches proposed in Ref. 3. With any of these approaches, the system is always stable because it is a type-II variable-stiffness system as shown in Ref. 3.

Equation of Motion and New Control Logic

As shown in Ref. 3, the equation of motion of the type-II on-off variable-stiffness system in modal coordinate is

$$\ddot{q} + \Omega q = g_0 + Gq \tag{1}$$

where

$$\Omega \equiv \mathrm{diag}\left(\omega_i^2\right) \tag{2}$$

$$g_0 \equiv \sum_{j=1}^{n_a} s_j \Phi^T \Delta K_j \Phi q_{0j} \tag{3}$$

$$G \equiv \sum_{j=1}^{n_a} (1 - s_j) \Phi^T \Delta K_j \Phi \tag{4}$$

$$\Phi \equiv [\phi_1, \phi_2, \ldots, \phi_n] \tag{5}$$

and q is the displacement vector in the modal coordinate, ω_i and ϕ_i are the angular frequency and mode shape of the ith mode of the full-stiffness system, respectively, ΔK_j is the decrement of the stiffness matrix in the physical coordinates due to stiffness reduction of the jth active member, s_j is the drive signal to the jth variable-stiffness element (stiffness is high when $s_j = 1$, and it is low when $s_j = 0$), q_{0j} is the displacement vector at the final stiffness recovery of the jth variable-stiffness element, and n_a is the number of variable-stiffness elements. The external force is assumed to be absent.

The variation of the stiffness matrix due to the stiffness reduction of the jth variable-stiffness truss member can be written as

$$\Delta K_j = \Delta k_j c_j c_j^T \tag{6}$$

where Δk_j is the scalar value of the stiffness reduction of jth member, c_j is the augmented c_{jE} into a large-size vector that includes the entire degrees of freedom of the system, c_{jE} is defined as

$$c_{jE} \equiv \lfloor c_{j1}, c_{j2}, c_{j3}, -c_{j1}, -c_{j2}, -c_{j3} \rfloor^T \tag{7}$$

and c_{ji} is the directional cosine between the jth member and ith axis of the global coordinates. Therefore, when the stiffness is high, Eq. (3) can be rewritten as follows by substituting $s_j = 1$ and Eq. (6) into it:

$$g_0 = \sum_{j=1}^{n_a} \Delta k_j \Phi^T c_j c_j^T \Phi q_{0j} \tag{8}$$

Next, let us introduce the following variables:

$$B \equiv \Phi^T \left[\Delta k_1 c_1, \Delta k_2 c_2, \ldots, \Delta k_{n_a} c_{n_a}\right] \tag{9}$$

$$u \equiv \left\lfloor u_1, u_2, \ldots, u_{n_a} \right\rfloor^T \tag{10}$$

$$u_j \equiv c_j^T \Phi q_{0j} \tag{11}$$

Then, when the stiffness is high, the equation of motion (1) can be rewritten as

$$\ddot{q} + \Omega q = Bu \tag{12}$$

This equation shows that we could apply the well-developed linear control theories if we could directly control u of this system. In LQ control theory, it is known[5] that the optimal linear control that minimizes

$$J \equiv \int_0^\infty \left(z^T R_1 z + u^T R_2 u\right) \mathrm{d}t \tag{13}$$

is to control u as

$$u = u_t \equiv -Fz \tag{14}$$

where

$$z \equiv \lfloor q, \dot{q} \rfloor^T \tag{15}$$

$$F = R_2^{-1} B^T P \tag{16}$$

and P is the positive-definite solution of the following Riccati equation:

$$PB^T R_2^{-1} BP - A^T P - PA - R_1 = 0 \tag{17}$$

In the present case, we cannot directly control u. But the preceding investigation suggests that a promising approach for vibration suppression of the present system is to reduce the stiffness for a short time only when the value of u_j is expected to become closer to u_{tj} by the stiffness reduction action. The value of u_j at the present time is given by Eq. (11). If the stiffness of the jth element is reduced

Received Jan. 27, 1993; revision received Aug. 3, 1995; accepted for publication Aug. 21, 1995. Copyright © 1995 by the American Institute of Aeronautics and Astronautics, Inc. All rights reserved.

*Professor, Research Division of Space Transportation, Yoshinodai. Member AIAA.

†Associate Professor, Research Division of Space Transportation, Yoshinodai. Member AIAA.

for a short time at the present moment and subsequently recovered, the value of u_j will become approximately

$$u_{aj} = c_j^T \Phi q \tag{18}$$

because the value of q after the stiffness recovery will be approximated by the present value of q. Therefore, we can see that the stiffness should be reduced when u_{aj} is more close to u_{tj} than u_j. But we should take account of another fact. In the LQ control, a large value of u results in a large penalty as shown by the term R_2 in Eq. (13). But in the present system, no penalty should be introduced for large value of u because it does not require large energy. Therefore, let us modify the aforementioned approach, and let us control the stiffness such that the absolute value of u_j becomes maximum when the signs of u_j and u_{tj} are the same; otherwise it becomes minimum. It can be implemented by reducing the stiffness of the jth element when

$$u_{tj}(u_{aj} - u_j) > 0 \tag{19}$$

and recovering it when

$$u_{tj}\dot{u}_{aj} \leq 0 \tag{20}$$

is held. In this Note, this approach is called as linear quadratic stiffness control (LQSC) after LQ control.

Numerical Investigation and Comparison with Other Approaches

Let us consider the five-bay truss structure shown in Fig. 1 as an example. The axial stiffness (EA) and the mass per unit length of each truss member are unity. The length of the members is also unity except for the diagonal members. In the bottom bay, three variable-stiffness members are installed. The amount of the stiffness reduction of these variable-stiffness members is limited to a half of nominal stiffness as

$$\Delta k_j = EA_j/(2l_j) \tag{21}$$

In the following investigation, the response of the structure to the unit impulse shown in Fig. 1 is simulated by numerically integrating Eq. (1). In the equation of motion, the entire 60 modes are included. The damping ratio of 0.5% is assumed for each mode.

To comparatively study the performance of the present approach, we also investigated two types of control logic proposed in Ref. 3 in addition to the present approach. Logic C proposed in Ref. 3 is to reduce the stiffness of each variable-stiffness member when the load on itself is at a maximum. In this Note, this approach is called the maximum load (ML) approach. This approach is suitable for decentralized control because the control logic is based on the locally available information only. The simplicity of the logic is also an advantage of the ML approach. Logic D proposed in Ref. 3 is to reduce the stiffness when the expected benefit is at a maximum. In this Note, this approach is called the maximum benefit function (MBF) approach. In Ref. 3, the MBF approach showed slightly higher performance than ML, although it is more complicated than ML.

Figure 2 shows a simulation result of vibration suppression by LQSC. In the figure, the responses of the lowest six modes are shown. To show the effects of higher modes, δ_{rms} is also shown, which is the root-mean-square value of the displacements of the nodes of truss. The value of

$$I = \int_0^\tau \delta_{\text{rms}}\, \mathrm{d}t \tag{22}$$

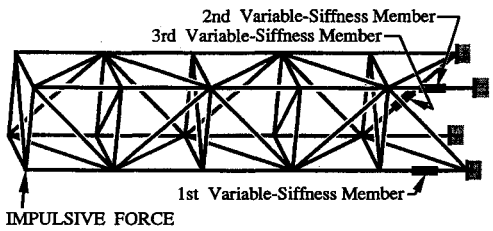

Fig. 1 Beamlike truss with variable-stiffness members.

Table 1 Values of I from various approaches and the roughly optimal parameter values

Approach	I	Parameter values
LQSC	145.0	$R_2 = 2 \times 10^4 \omega_1^2$
ML	348.2	$\tau_f = 2, \tau_c = 10$
MBF	122.4	$\tau_f = 2, \tau_c = 2, \tau_d = 10$
No control	564.4	——

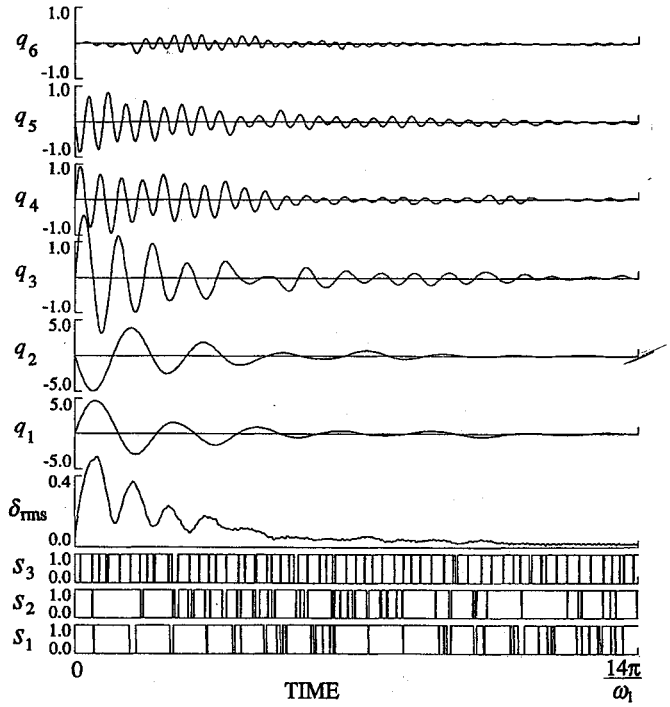

Fig. 2 Simulation result of vibration suppression by LQSC.

is also shown in Table 1, where τ is seven cycle periods of the lowest natural frequency of the full stiffness structure. In this simulation, the lowest six modes are controlled. The value of R_1 is set such that $z^T R_1 z$ represents the total energy of the system. The value of R_2 that minimizes I is roughly optimized, and it is set as $R_2 = 2 \times 10^4 \omega_1^2$. It is interesting that a further lower value of R_2 does not result in a lower value of I, although the gain in the LQ control system increases. The sixth mode, which is not excited by the impulse, is once excited by the control action. This is due to an energy transfer from other modes. However, it is suppressed soon as the other modes are suppressed, from which energy can be transferred. The figure shows that all of the modes, especially the lowest two modes, are suppressed nicely.

The other two approaches from Ref. 3, ML and MBF, are also applied. The values of the parameters τ_f, τ_c, and τ_d are roughly optimized for each approach. The parameter values and the value of I for each approach are shown in Table 1. The value of I without any control is also listed for the reference. The table shows that the performance of LQSC is much higher than ML, whose logic is simple and suitable for decentralized control. The performance of MBF is much higher than ML, although difference was small in the example shown in Ref. 3. It can also be seen that the performance of LQSC is slightly lower than that of MBF, whose logic is more complicated than that of LQSC.

Concluding Remarks

Suggested by LQ control theory, a new control logic, LQSC, has been proposed for the vibration suppression of the MDOF structure with multiple type-II variable-stiffness members. To investigate the performance of the proposed approach, the vibration suppression of a truss structure has been numerically simulated. Simulation results have shown that the newly proposed approach suppresses the vibration nicely by controlling the stiffness. Comparison with two

other known approaches, ML and MBF, has shown that the performance of LQSC is much higher than that of ML. The performance of LQSC is slightly lower than that of MBF, although the control logic is simpler than that of MBF. It should be noted that, as shown in Ref. 3, the system with any of these approaches is always stable because it is the type-II variable-stiffness system.

References

[1]Chen, J.-C., "Response of Large Space Structures with Stiffness Control," *Journal of Spacecraft and Rockets*, Vol. 21, No. 5, 1984, pp. 463–467.

[2]Fanson, J. L., Chen, J.-C., and Caughey, T. K., "Stiffness Control of Large Space Structures, Control of Flexible Space Structures," Jet Propulsion Lab., JPL Publication 85-29, California Inst. of Technology, Pasadena, CA, April 1985, pp. 351–364.

[3]Onoda, J., Endo, T., Tamaoki, H., and Watanabe, N., "Vibration Suppression by Variable-Stiffness Members," *AIAA Journal*, Vol. 29, No. 6, 1991, pp. 977–983.

[4]Minesugi, K., "Vibration Control of Flexible Structures by Variable Axial Stiffness Active Members," Ph.D. Dissertation, Dept. of Aeronautics, Univ. of Tokyo, Japan, Dec. 1990 (in Japanese).

[5]Kwakernaak, H., and Sivan, R., *Linear Optimal Control System*, Wiley-Interscience, New York, 1972.

Structure and Properties of Three-Dimensional Braided Composites Including Axial Yarns

Soheil Mohajerjasbi*
Boeing Defense and Space Group,
Philadelphia, Pennsylvania 19142-0858

Introduction

TEXTILE preforming and resin transfer molding (RTM) have been identified among the manufacturing processes that offer the potential to make composite structures cost effective compared with aluminum structures. The potential of textile composites in reducing cost is envisioned in the ability to manufacture near-net-shape parts and the use of fiber and matrix in their lowest cost form. The cost-saving potential of textile composites is realized when the process of preform fabrication is automated and therefore the labor-intensive process of laying up the laminate or the dry fabric by hand is eliminated.

One such textile preforming process is three-dimensional Cartesian braiding that produces three-dimensional preform. A wide range of complex geometric shapes may be produced by this process. Other advantages of this class of composites include delamination resistance and good energy absorption capability. The process is not without limitations, however; presently available braiding machines are not fully automated, are relatively slow, and the size of the parts that can be produced with this process is limited by the physical dimensions of the braiding machine.

Any attempt to model the thermoelastic properties of this class of composites should take into account the structure of the preform, which is much different from the conventional laminated composites.

Fiber Architecture

A braiding machine, schematically shown in Fig. 1, is used to fabricate three-dimensional braided preforms. The yarn carriers that

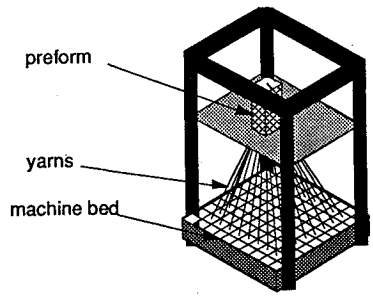

Fig. 1 Schematic of a three-dimensional Cartesian braiding machine.

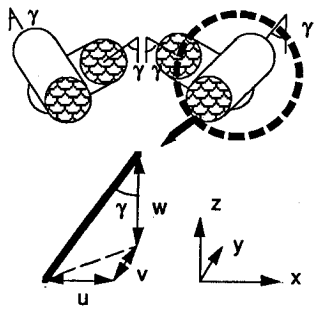

Fig. 2 Yarn arrangement in the interior of three-dimensional braided composite.

are loaded with yarns are arranged in rows and columns on the machine bed to form a shape similar to the shape of the preform to be produced. The ends of the yarns are tied to a movable plate above the braiding machine. Movements of the yarn carriers on the machine bed in a prescribed manner will produce the braided preform above the machine. The number, arrangement, and the movements of the yarn carriers on the machine bed determine the fiber architecture of the preform. The braiding process that is considered here is referred to as (1 × 1) or four-step process. In the four-step process, similar yarn carrier configuration is obtained after every four machine steps, and therefore the fiber architecture of the preform is a repetition of the fiber architecture produced in four machine steps. This yarn structure is referred to as repeat unit. It is possible to add stationary yarns on the machine that do not participate in these carrier movements. These yarns will remain parallel to the braiding axis, and the resulting preform will have axial yarns that are directed along the length of the preform.

In the following, the fiber architecture of the repeat unit is briefly reviewed. More detailed explanation of the yarn carrier movements and the resulting fiber architecture of the preform may be found in Ref. 1.

In every two machine steps, as a result of the movements of the yarn carriers on the bed of the braiding machine, the yarns in the interior of the preform produce two different yarn formations that are characterized by interior braiding angle γ with respect to the axis of the braided preform (z axis). These two yarn formations, which are shown in Fig. 2, are not identical, but a symmetry exists between them. These two yarn formations alternate along 45 and 135 deg measured from the preform x axis and along the axis of the braided preform (z axis). The movements of the carriers resulting in formation of the boundary and corners are different; therefore the fiber architectures at the corners and the boundaries are different from the interior. The fiber architectures at the boundaries and corners of the preform are also demonstrated in Ref. 1. The interior braiding angle γ cannot be measured directly without cutting the preform; however, it can be calculated from orientation angle of the yarns on the surface of the composite, which is referred to as surface angle. A relationship exists between the interior braiding angle, the surface angle, and the parameters u, v, and w shown in Fig. 2. Equations establishing the relationship between the interior braiding angle, the surface angle, and the parameters u, v, and w may be found in Refs. 1 and 2.

The three parameters u, v, and w completely describe the geometry of the interior, boundaries and the corners of the preform. Since the fiber architecture of the preform is the repeat of the yarn

Received Feb. 13, 1995; revision received Sept. 5, 1995; accepted for publication Sept. 14, 1995. Copyright © 1995 by The Boeing Co. Published by the American Institute of Aeronautics and Astronautics, Inc., with permission.

*Staff Engineer, Helicopters Division, P.O. Box 16858, MS P38-13. Member AIAA.